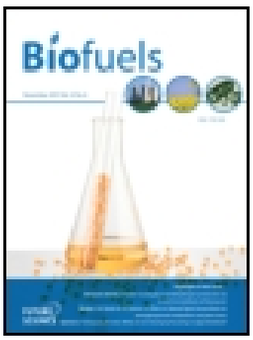

Biofuels

ISSN: 1759-7269 (Print) 1759-7277 (Online) Journal homepage: http://www.tandfonline.com/loi/tbfu20

Investigation of the slow pyrolysis kinetics of oil palm solid waste by the distributed activation energy model

Fredy Surahmanto, Harwin Saptoadi, Hary Sulistyo & Tri Agung Rohmat

To cite this article: Fredy Surahmanto, Harwin Saptoadi, Hary Sulistyo & Tri Agung Rohmat (2017): Investigation of the slow pyrolysis kinetics of oil palm solid waste by the distributed activation energy model, Biofuels, DOI: 10.1080/17597269.2017.1387750

To link to this article: http://dx.doi.org/10.1080/17597269.2017.1387750

Published online: 27 Oct 2017.

BIOFUELS, 2017
https://doi.org/10.1080/17597269.2017.1387750

Taylor & Francis
Taylor & Francis Group

Investigation of the slow pyrolysis kinetics of oil palm solid waste by the distributed activation energy model

Fredy Surahmanto[a], Harwin Saptoadi[a], Hary Sulistyo[b] and Tri Agung Rohmat[a]

[a]Department of Mechanical and Industrial Engineering, Universitas Gadjah Mada, Indonesia; [b]Department of Chemical Engineering, Universitas Gadjah Mada, Indonesia

ABSTRACT

Oil palm solid waste has promising potential as future feedstock for bioenergy generation due to its abundant availability as an impact of the increasing world's palm oil production. In this study, non-isothermal thermogravimetry measurements under an inert atmosphere of nitrogen were conducted at heating rates of 5, 10, 15 and 20°C/min, on oil palm solid waste, including its components: empty fruit bunch (EFB), fibre, and shell. The distributed activation energy model (DAEM) was used to investigate the pyrolysis kinetic parameters, comprising activation energy and frequency factor. The activation energy and frequency factor values for EFB, fibre, and shell are from 107.17 to 227.28 kJ/mol and from 1.79E+13 to 9.87E+20 s^{-1}; from 50.75 to 213.22 kJ/mol and from 8.40E+05 to 4.25E+15 s^{-1}, and from 59.36 to 170.30 kJ/mol and from 1.54E+07 to 1.11E+14 s^{-1}, respectively. It was found that the activation energy values of all components vary with the progress on conversion, and they show different trends. The DAEM can be used to determine the pyrolysis kinetic parameters and provides reasonable fit to the experimental data.

ARTICLE HISTORY
Received 28 May 2017
Accepted 18 September 2017

KEYWORDS
Oil palm solid waste; pyrolysis; kinetics; the DAEM

Introduction

At present, large-scale oil palm plantations have been intentionally expanded for palm oil production by extracting the flesh part and the innermost nut of the palm fruit. As a consequence of the production increase, the quantity of oil palm solid waste, including empty fruit bunch (EFB), fibre, shell and kernel, will certainly be abundant.

For every ton of palm oil produced from fresh fruit bunches, approximately 1 ton of EFB, 0.7 ton of palm fibres, 0.3 ton of palm kernels and 0.3 ton of palm shells remain [1]. By this approximation, it can be estimated that for world's oil palm production in 2017 of 66.86 million metric tons [2], the total biomass generated from the palm oil industry would be around 153.778 million metric tons.

To hinder environmental threats, of course, appropriate handling and utilisation are needed for this large amount of biomass. So, these renewable energy materials could be used as alternatives for producing valuable chemical products by applying thermochemical conversion processes, including pyrolysis, combustion, or gasification [3–5].

Pyrolysis is a promising process for biomass upgrading by cracking the polymer structure of lignocellulosic materials and converting them into a volatile fraction consisting of gases, vapours, tar components and char [6,7]. Knowledge and understanding of pyrolysis kinetics of biomass are needed to properly design and establish an efficient and safe process [8–11].

The activation energy and the frequency factor are the main parameters to describe biomass pyrolysis kinetics. Several different kinetics models have been proposed for the lignocellulosic biomass pyrolysis process, including independent parallel reactions [12], isoconversional methods [13], three-parallel Gaussian reaction [14] and the distributed activation energy model (DAEM) [15]. Among these models, the DAEM was successfully applied to different biomass fuels for understanding the reaction kinetics of the pyrolysis process [15,16]. It has been proved an accurate method to describe the pyrolysis kinetics of biomass, obtaining good agreement with the experimental data [17]. Moreover, it has been widely used to analyse complex reactions that occur during fossil fuel pyrolysis [18,19].

Nevertheless, the study of oil palm solid waste using DAEM is still limited. Therefore, this study aimed to investigate the pyrolysis behaviour of oil palm solid waste – EFB, fibre and shell – at different heating rates, and determine the distributed activation energy (E) and frequency factor (A) corresponding to different mass conversions.

Material and methods

Raw material

Oil palm solid waste, including EFB, fibre and shell, used in this study was obtained from a palm oil mill. Prior to experiments conducted, these materials were

CONTACT Fredy Surahmanto fredy.surahmanto@mail.ugm.ac.id

crushed and sieved into particles sized 0.21 mm. Then, proximate, ultimate, and fibre analysis were done to these samples, with results as shown in Table 1.

Thermogravimetry experiment

Thermogravimetry experiments were conducted with an automatic simultaneous thermal analyser, which provides simultaneous thermogravimetry (TG) and differential thermal analysis (DTA) on a single sample (Shimadzu, DTG–60, Japan; with temperature accuracy of 0.1 K, DTA sensitivity of 0.1 μV and TG sensitivity of 1 μg). For every run, about 8 mg of sample with particle size of 0.21 mm was used, and 15 mL/min nitrogen was flowed to provide an inert atmosphere. Heating rate variations of 5, 10, 15 and 20°C/min were applied, and an initial temperature of 30°C, a final temperature of 550°C, and then a holding time of 20 min were set. The final temperature was considered to be the optimum temperature during slow pyrolysis, in which the optimum yields of all pyrolysis products can be reached [20–22], so that it will be useful to the related findings. The instrument provided continuous recording of TG and DTA curves and data that were used to calculate the kinetic parameters. Each experiment was repeated at least twice to ensure its reproducibility.

The distributed activation energy model (DAEM)

The DAEM assumes that a number of irreversible first-order parallel reactions that have different kinetic parameters take place simultaneously. The change of total volatile at time t can be expressed as:

$$1 - \frac{V}{V^*} = \int_0^\infty \exp\left(-A\int_0^t e^{-E/RT}dt\right) f(E)dE \quad (1)$$

Where V^* and V represent effective volatile content and volatile content at temperature T, $f(E)$ is the distribution curve of activation energy which represents the activation energy difference of all reactions, and A is a frequency factor corresponding to the activation energy value. In this study, an integral method proposed by Miura and Maki [18] was used to estimate the kinetic parameters. Then, Equation (1) can be rewritten as:

$$1 - \frac{V}{V^*} = \int_0^\infty \text{Ø}(E,T) f(E)dE \quad (2)$$

$$\text{where } \text{Ø}(E,T) = \exp\left(\frac{-A}{\beta}\int_0^T e^{-E/RT}dT\right) \quad (3)$$

$$\text{Ø}(E,T) \cong \exp\left[\frac{-ART^2}{\beta E}e^{-E/RT}\right] \quad (4)$$

where β is a constant heating rate.

Since the Ø(E, T) function changes steeply with activation energy at a given temperature, it is approximated by a step function at $E = E_s$. This approximation corresponds to the assumption that the single reaction with activation energy E_s is occurring at temperature T. Thus, Equation (1) can be simplified as:

$$\frac{V}{V^*} \cong 1 - \int_{E_s}^\infty f(E)dE = \int_0^{E_s} f(E)dE \quad (5)$$

The activation energy, E_s is chosen to satisfy $\text{Ø}(E_s, T) = 0.58$. The relationship of E_s to β, T, and A is given as:

$$0.545\beta E_s / ART^2 = e^{-Es/RT} \quad (6)$$

This treatment approximates that a reaction with activation energy E_s occurs at a specified temperature T and a constant heating rate β. The approximation is mathematically given by:

$$\frac{dV}{dt} \cong \frac{d(\Delta V)}{dt} = Ae^{-E/RT}(\Delta V^* - \Delta V) \quad (7)$$

This equation shows that the overall dV/dt is approximated by the rate of specific reaction only at the temperature at which the reaction is occurring. The ΔV and ΔV^* are the amount of volatiles and the effective volatile content for the same reaction, respectively.

By integrating Equation (7), and applying the Ø function approximation, the resulting equation can be represented as:

$$1 - \frac{\Delta V}{\Delta V^*} = \exp\left(-k_0\int_0^t e^{-E/RT}dt\right) \cong \exp\left(\frac{-k_0RT^2}{\beta E}e^{-E/RT}\right) \quad (8)$$

Natural logarithm was applied to both sides of Equation (8), so that:

$$ln\left(\frac{\beta}{T^2}\right) = ln\left(\frac{k_0R}{E}\right) - ln\left(-ln\left(1 - \frac{\Delta V}{\Delta V^*}\right)\right) - \frac{E}{RT} \quad (9)$$

Equation (9) is the integral form of the basic equation, and by substituting $1 - \Delta V/\Delta V^*$ with 0.58, the equation is simplified as:

$$ln\left(\frac{\beta}{T^2}\right) = ln\left(\frac{k_0R}{E}\right) + 0.6075 - \frac{E}{RT} \quad (10)$$

Using Equation (10), the activation energy and frequency factor are determined from the slope and intercept of the Arrhenius plot of ln (β/T^2) vs. 1/T at selected values of V/V^* at different heating rates.

Results and discussion

Thermal degradation behaviour

Figure 1 shows the TG and derivative thermogravimetry (DTG) curves of EFB, fibre and shell, at different heating rates of 5, 10, 15, and 20°C/min. It can be observed from Figure 1(a) that in the temperature range between 30 and 220°C, EFB underwent small mass loss with maximum mass loss rate as 1.55, 2.45, 3.68, and 4.75%/min, at temperatures of 120, 137, 143, and 154°C, respectively. Then, continuing to the main devolatilisation stage up to around 400°C, it reached a maximum loss rate of 3.10, 6.44, 8.95 and 11.82%/min, at temperatures of 311, 328, 329, and 344°C, respectively.

Figure 1(b) shows that small mass loss with maximum mass loss rate of 0.71, 1.6, 2.46, and 3.07%/min occurred at 106, 116, 123, and 142°C, respectively, in the moisture evaporation stage of fibre in the temperature range between 30 and 207°C. In the next stage, up to 430°C, two peaks of mass loss rate appeared in DTG curves, with first peaks of 1.93, 4.24, 5.83, and 7.74%/min occurring at 272, 286, 292, and 311°C, respectively. The second peaks of 2.46, 5.09, 6.43, and 8.30%/min happened at 335, 345, 352, and 371°C, respectively.

As shown by Figure 1(c), maximum mass loss rate of 0.87, 1.94, 2.62, and 4.39%/min occurred at 106, 119, 122, and 133°C, respectively, in the moisture evaporation stage of shell, from 30 to around 220°C. In the next stage, similar to fibre, two peaks of mass loss rate were observed for shell, with first peaks of 2.30, 4.53, 6.87, and 9.61%/min at 267, 280, 292, and 303°C, respectively. Then, second peaks of 2.94, 5.88, 8.06, and 9.40%/min happened at 345, 358, 366, and 383°C, respectively.

It can be clearly seen that heating rate had an effect on the temperature range of the pyrolysis stages. The TG and DTG curves shifted towards the higher temperature range with the increase of heating rate. The maximum rate of decomposition tends to increase at higher heating rates because there is more thermal energy to enable better heat transfer between the surroundings and the insides of the samples. In addition, the temperature corresponding to this maximum mass loss, T_{max}, was also increased. In more detail, there were some differences in the T_{max} among these three components. At the moisture evaporation stage, it was observed that EFB has the highest T_{max}, while at the devolatilisation stage, the second T_{max} of shell was significantly higher than that of fibre. This could be possibly attributed to the amounts of minerals present in each sample, as suggested by previous research conducted by Vamvuka and Sfakiotakis [10] on other biomass, including giant reed, switchgrass and cardoon.

Furthermore, only one mass loss peak appeared in the devolatilisation of EFB, with a small shoulder located at the lower temperature side. The shoulder probably represents the decomposition of hemicellulose present in the material, and the higher

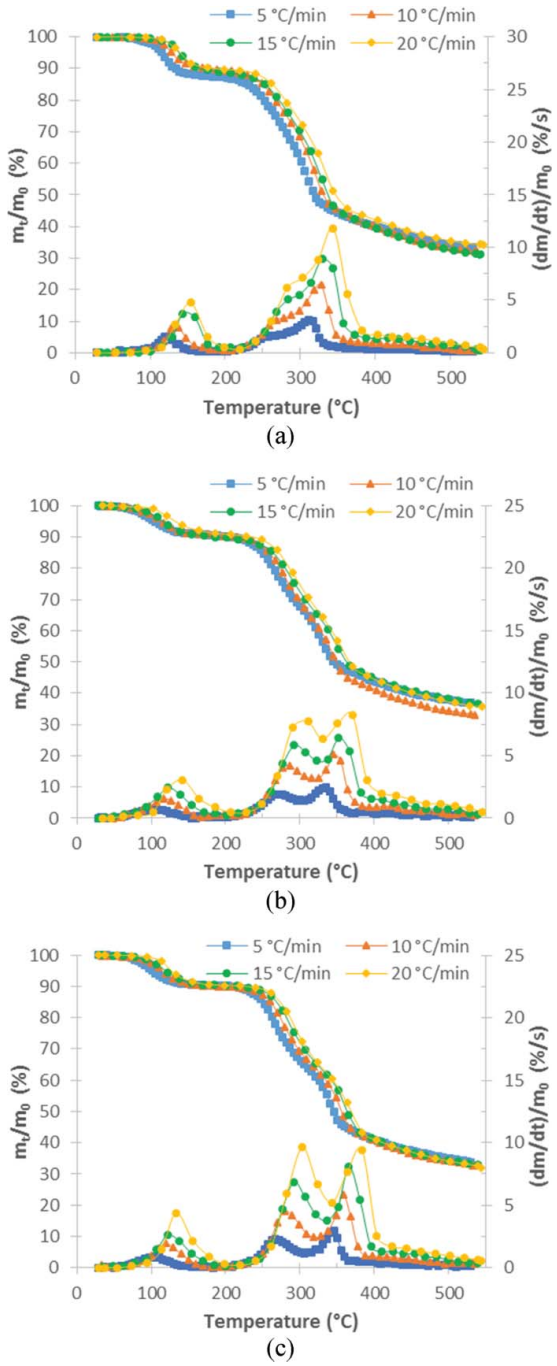

Figure 1. Thermogravimetric (TG) and derivative thermogravimetric (DTG) curves of oil palm solid waste: (a) empty fruit bunch (EFB), (b) fibre, and (c) shell at different heating rates.

temperature peak corresponds to the decomposition of cellulose [23]. Moreover, the decomposition rate of hemicellulose in EFB is greater than that of cellulose, while for fibre and shell the decomposition rate of cellulose is dominant. A single peak with a small shoulder of the DTG curve was also found for the pyrolysis of olive kernel [23] and poplar wood [24].

Kinetic analysis of the pyrolysis process

The kinetic parameters according to the degree of solid conversions are determined by the procedure as follows [18]:

- Measure V/V^* vs. T relationships at different heating rates.
- Calculate the values of (β/T^2) and $(1/T)$ at the same V/V^* values from V/V^* vs. T relationships at different heating rates.
- Plot ln (β/T^2) vs. $(1/T)$ at the same V/V^* value and determine the E (from the slope) and A (from the intercept) values from the Arrhenius plots at different V/V^* using the relationship in Equation (10).

Following that procedure, TG tests that have been conducted at 5, 10, 15, and 20°C/min resulted in conversion rate plotted in Figure 2 for each heating rate. It can be clearly seen that the conversion occurs at higher temperatures when the heating rate increases. Hence, the temperature at which each conversion rate takes place can be obtained from Figure 2, for each heating rate. Then, with these temperatures, an Arrhenius plot for EFB, fibre and shell of oil palm solid waste can be drawn, by plotting ln (β/T^2) vs. $(1/T)$ as shown by Figure 3 for each conversion rate, with variations of 10%.

The Arrhenius plot for EFB is relatively linear and parallel at conversion from 0.3 to 0.7, and this gives an average value of activation energy of 168 kJ/mol. However, outside this range, the plot behaves differently. As can be seen in Figure 4(a), the activation energies and frequency factors vary from 107.17 to 227.28 kJ/mol and from 1.79E+13 to 9.87E+20 s^{-1}, respectively. The lowest value of activation energy took place at the conversion of 0.1, in a temperature range between 128 and 145°C, which is in the moisture evaporation stage. In contrast, the highest one took place at the conversion of 0.9, in a temperature range between 407 and 430°C, which is in the pyrolysis stage.

A relatively linear and parallel Arrhenius plot was also obtained for the oil palm fibre at conversion from 0.3 to 0.7 and this gives an average value of activation energy of 165 kJ/mol, as depicted in Figure 4(b). Similar to the EFB, the fibre had the lowest and highest activation energy values at the conversion of 0.1 (taking place from 114 to 146°C) and 0.9 (taking place from 418°C to 442°C), respectively.

Slightly different from the EFB and the fibre, as can be seen in Figure 4(c), the oil palm shell has the highest activation energy, of 170.3 kJ/mol at the conversion of 0.6 (which took place from 326 to 349°C). The Arrhenius plot in Figure 3(c) is shown to be linear and relatively parallel at the conversion from 0.1 to 0.8. The coefficient of correlations (R^2) of all components for all lines drawn at various conversions (from 0.1 to 0.9), which is greater than 0.90, indicates the best fit.

As shown by Figure 5, the highest activation energy values at various conversions reached 227.28, 213.22, and 170.30 kJ/mol for EFB, fibre and shell, respectively. These were followed by the corresponding frequency factor values of 4.66E+16, 2.21E+15, and 1.11E+14 s^{-1}.

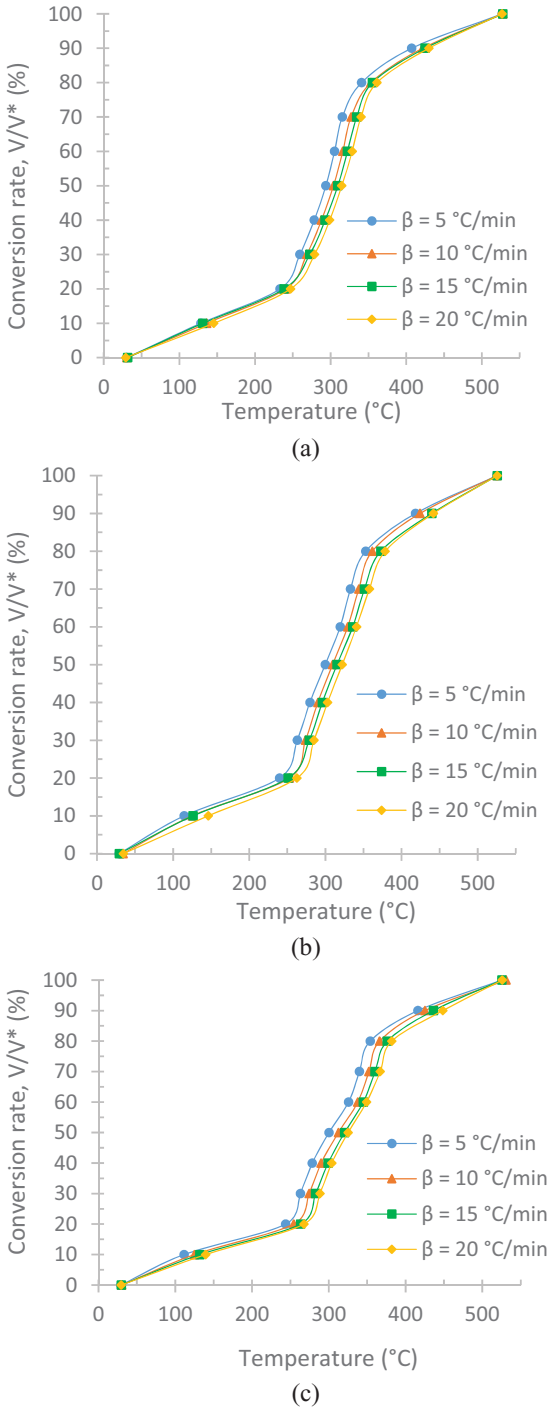

Figure 2. Conversion rate vs. temperature for each heating rate on (a) empty fruit bunch (EFB), (b) fibre, and (c) shell.

It is obvious that the activation energy of shell is relatively lower than that of the other two components. This implies that shell requires less energy to break down the chemical bonds between atoms, and its reaction rate is faster than the others. In more detail, the values of activation energy and frequency factor for slow pyrolysis on all components of oil palm solid waste are presented in Table 2.

This can be related to the three main constituents of lignocellulosic biomass: hemicellulose, cellulose, and lignin. As presented in Table 1, the proportions of cellulose, hemicellulose, and lignin in the shell are 15.54,

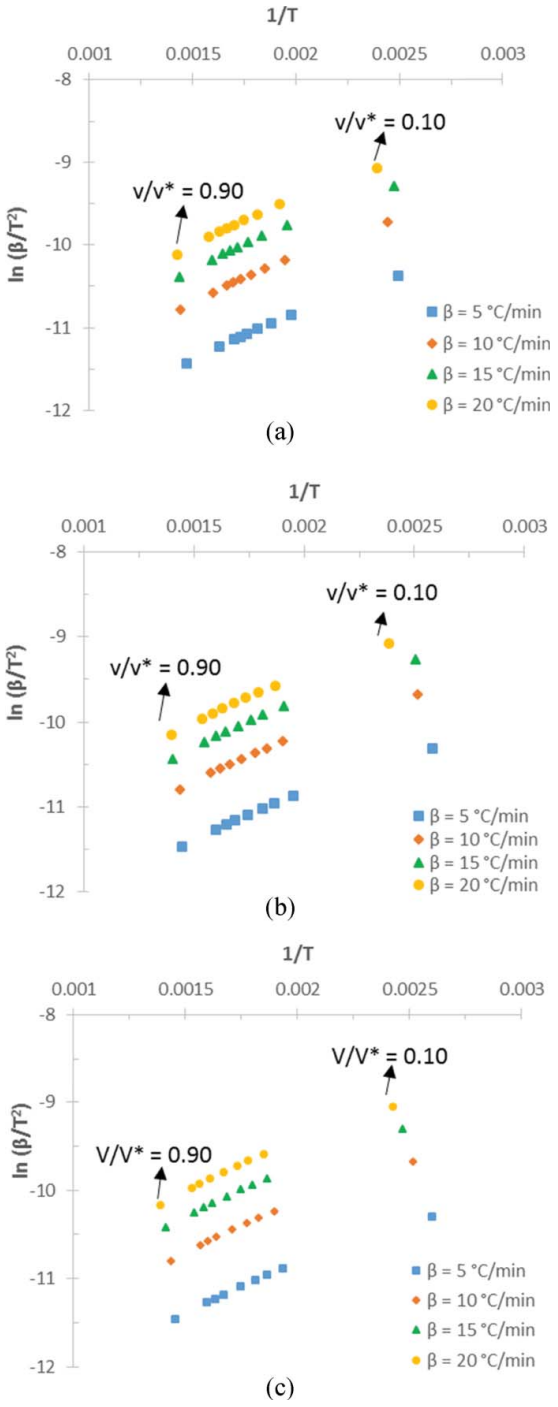

Figure 3. Arrhenius plot for (a) empty fruit bunch (EFB), (b) fibre and (c) shell.

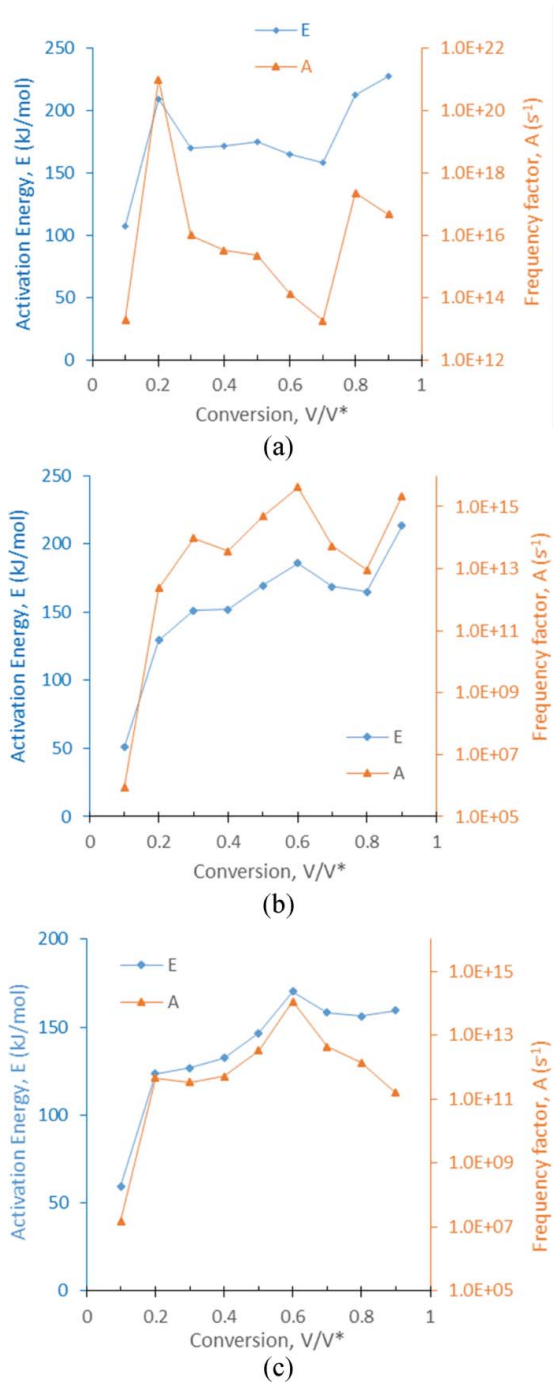

Figure 4. The activation energy and frequency factor values of (a) empty fruit bunch (EFB), (b) fibre and (c) shell, at different conversion rate.

35.79, and 36.96 wt. %, respectively, indicating that the lignin contents are high and the cellulose contents are low. Inversely, the cellulose contents are high and lignin contents are low in EFB and fibre. In more detail, the proportions of cellulose, hemicellulose, and lignin in EFB are 20.15, 35.01, and 19.65 wt. %, whereas the corresponding contents in the fibre are 23.99, 37.67, and 22.99 wt. %.

These composition analysis results are similar to those found by previous studies. Shibata et al. [25] reported that the proportions of cellulose, hemicellulose and lignin in the shell were 20.5, 22.3 and 51.5%, respectively. In addition, the corresponding percentages in the fibre (mesocarp) and EFB were 39.5% and 37.9%; 9.8% and 35.0%; and 32.8% and 22.9%, respectively. In contrast, Mae et al. [26] reported that oil palm shell consists of 31% cellulose, 20% hemicellulose and 49% lignin. Furthermore, Abdullah and Sulaiman [27] found that EFB consists of 57.8% cellulose, 21.2% hemicellulose and 22.8% lignin. These values are in the percentage intervals determined by Chang [1], that EFB comprises 24–65% cellulose, 21–

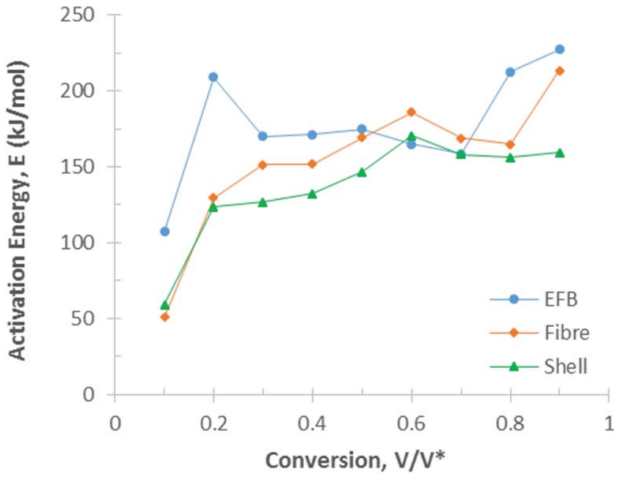

Figure 5. Comparison of activation energy vs. conversion from the Arrhenius plot. EFB: empty fruit bunch.

Table 1. Proximate, ultimate and composition analysis of oil palm solid waste.

Component	EFB	Fibre	Shell
Proximate analysis (wt. %)			
Moisture content	8.503	7.736	7.630
Volatile matter	62.431	62.668	63.356
Fixed carbon	22.004	23.521	27.976
Ash	7.062	6.075	1.038
Higher heating value (cal/g)	3757.582	4359.673	4781.011
Ultimate analysis (wt. %)			
Carbon	40.63	42.93	49.01
Hydrogen	6.11	6.09	6.18
Nitrogen	1.23	1.15	0.27
Sulphur	0.14	0.14	0.04
Oxygen	44.80	42.56	43.46
Composition analysis (wt. %)			
Hemicellulose	20.15	23.99	15.54
Cellulose	35.01	37.67	35.79
Lignin	19.65	22.99	36.96

EFB: empty fruit bunch.

34% hemicellulose and 14–31% lignin. This study revealed that lignin content in oil palm shell is the highest among the three components, whereas the cellulose contents is dominant in EFB.

The previous studies found that each of the components decomposed at a different temperature range [10,28,29]. In more detail, Vamvuka et al. [10] found that lignin started to decompose at a low rate and low temperature of about 200°C, continuing to 600°C. Thus, it decomposed in both active and passive pyrolysis zones. In contrast, hemicellulose decomposed between 200 and 350°C. Finally, cellulose decomposed at a higher temperature range, of 280–400°C.

Meanwhile, Yang et al. [29] found that hemicellulose started decomposing easily, with the weight loss mainly occurring from 220 to 315°C. Cellulose pyrolysis occurred at a higher temperature range (from 315 to 400°C). Lignin decomposed slowly, from the ambient temperature to 900°C.

These findings can be explained by the fact that cellulose is a semi-crystalline material, while hemicellulose and lignin are non-crystalline, so the pyrolysis of cellulose must first destroy the lattice structure of cellulose which takes extra energy, leading to higher activation energy [30,31]. The amorphous nature of hemicellulose causes it to be less stable than the others. Due to its strong inter-molecular hydrogen bonding, cellulose required higher activation energy than hemicellulose, whereas the complex structure with many oxygenated functional groups, and the scission of the associated bonds in lignin which can occur at different temperature ranges, caused varying thermal stability in lignin [32].

The activation energy values varied with the progress of conversion. In agreement with Ceylan and Kazan [6], this indicates that more than a single reaction mechanism is involved in the thermal decomposition of this oil palm solid waste.

In this work, the distribution function of activation energy, f(E), was used to describe the relationship between model parameters and kinetic data obtained from the experiments. This function can be obtained based on Figure 5, Equation (5) and the Gaussian distribution [33]. The function of activation energy vs. activation energy for EFB, fibre, and shell is depicted in Figure 6. It can be clearly seen that the Gaussian distribution function can describe the relationship between f(E) and E at high accuracy (R^2 = 0.99) for all components. This indicates that DAEM is capable of determining the pyrolysis kinetic parameters and provides reasonable fit to the experimental data.

Table 2. Values of activation energy, frequency factor and correlation factor of oil palm solid waste.

	EFB			Fibre			Shell		
V/V* (%)	E (kJ/mol)	A (s^{-1})	R^2	E (kJ/mol)	A (s^{-1})	R^2	E (kJ/mol)	A (s^{-1})	R^2
10	107.17	1.96E+13	0.9978	50.75	8.40E+05	0.9638	59.36	1.54E+07	0.9963
20	209.01	9.87E+20	0.9967	129.42	2.40E+12	0.9921	123.41	4.62E+11	0.9938
30	170.23	1.03E+16	0.9847	151.25	9.55E+13	0.9925	126.74	3.30E+11	0.9975
40	171.41	3.30E+15	0.9921	151.76	3.71E+13	0.9915	132.36	5.00E+11	0.9965
50	174.65	2.26E+15	0.9985	169.38	4.96E+14	0.9880	146.54	3.29E+12	0.9989
60	164.97	1.31E+14	0.9969	185.79	4.25E+15	0.9988	170.30	1.11E+14	0.9985
70	158.53	1.79E+13	0.9995	168.78	5.49E+13	0.9960	158.18	4.24E+12	0.9979
80	212.72	2.28E+17	0.9626	165.11	9.08E+12	0.9681	156.14	1.36E+12	0.9955
90	227.28	4.66E+16	0.9689	213.22	2.21E+15	0.9180	159.43	1.55E+11	0.9289

EFB: empty fruit bunch.

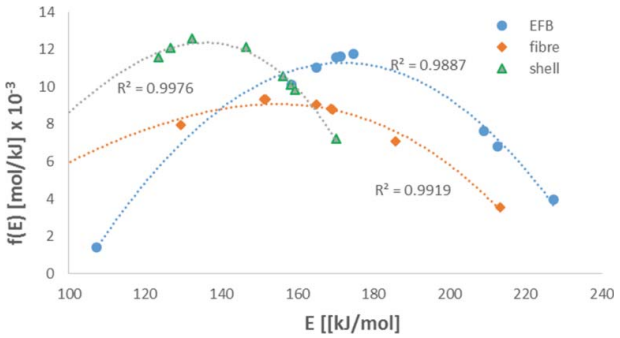

Figure 6. The relationship between f(E) and E. EFB: empty fruit bunch.

Conclusions

It was found that the activation energies of all components vary with the progress of conversion, and show different trends among components.

The lower activation energy of oil palm shell compared to those of the other components implies that less energy is required by shell to break down the chemical bonds between atoms, so its reaction rate is faster than the others.

The distributed activation energy model (DAEM) can be used to determine the pyrolysis kinetic parameters, and provides a reasonable fit to the experimental data.

Acknowledgements

The authors gratefully acknowledge the Ministry of Research, Technology and Higher Education of the Republic of Indonesia for financial support, and Mr Sudarto from the Institute of Plantation Education, Yogyakarta, for supplying the oil palm solid waste.

Disclosure statement

No potential conflict of interest was reported by the authors.

References

[1] Chang SH. An overview of empty fruit bunch from oil palm as feedstock for bio-oil production. Biomass and Bioenergy. 2014;62:174–181.
[2] U. S. D. of Agriculture. World's palm oil production. Washington, DC. 2017.
[3] Ly HV, Kim J, Kim SS. Pyrolysis characteristics and kinetics of palm fiber in a closed reactor. Renew Energy. 2013;54:91–95.
[4] Wang G, Li W, Li B, et al. TG study on pyrolysis of biomass and its three components under syngas . Fuel. 2008;87:552–558.
[5] Mckendry P. Energy production from biomass (part 2): conversion technologies. Bioresour Technol. 2002;83:47–54.
[6] Ceylan S, Kazan D. Bioresource Technology Pyrolysis kinetics and thermal characteristics of microalgae Nannochloropsis oculata and Tetraselmis sp. Bioresour Technol. 2015;187:1–5.
[7] Poletto M, Zattera AJ, Santana RMC. Thermal decomposition of wood: kinetics and degradation mechanisms. Bioresour Technol. 2012;126:7–12.
[8] El-Sayed SA, Mostafa ME. Pyrolysis characteristics and kinetic parameters determination of biomass fuel powders by differential thermal gravimetric analysis (TGA/DTG). Energy Convers Manag. 2014;85:165–172.
[9] Gai C, Dong Y, Zhang T. The kinetic analysis of the pyrolysis of agricultural residue under non-isothermal conditions. Bioresour Technol. 2013;127:298–305.
[10] Vamvuka D, Sfakiotakis S. Effects of heating rate and water leaching of perennial energy crops on pyrolysis characteristics and kinetics. Renew Energy. 2011;36:2433–2439.
[11] Mani T, Murugan P, Abedi J, et al. Pyrolysis of wheat straw in a thermogravimetric analyzer: effect of particle size and heating rate on devolatilization and estimation of global kinetics. Chem Eng Res Des. 2010;88:952–958.
[12] Rueda-ordóñez YJ, Tannous K, Olivares-gómez E. An empirical model to obtain the kinetic parameters of lignocellulosic biomass pyrolysis in an independent parallel reactions scheme. Fuel Process Technol. 2015;140:222–230.
[13] Brachi P, Miccio F, Miccio M, et al. Pseudo-component thermal decomposition kinetics of tomato peels via isoconversional methods. Fuel Process Technol. 2016;154:243–250.
[14] Chen T, Zhang J, Wu J, Kinetic and energy production analysis of pyrolysis of lignocellulosic biomass using a three-parallel Gaussian reaction model. Bioresour Technol. 2016;211:502–508.
[15] Sonobe T, Worasuwannarak N, .Kinetic analyses of biomass pyrolysis using the distributed activation energy model. Fuel. 2008;87:414–421.
[16] Shen DK, Gu S, Jin B, et al. Thermal degradation mechanisms of wood under inert and oxidative environments using DAEM methods. Bioresour Technol. 2011;102:2047–2052.
[17] Soria-Verdugo A, Garcia-Gutierrez LM, Blanco-Cano L, et al. Evaluating the accuracy of the distributed activation energy model for biomass devolatilization curves obtained at high heating rates. Energy Convers Manag. 2014;86:1045–1049.
[18] Miura K, Maki T. A simple method for estimating f(E) and ko(E) in the distributed activation energy model. Energy & Fuels. 1998;12:864–869.
[19] Navarro MV, Aranda A, Garcia T, et al. Application of the distributed activation energy model to blends devolatilisation. Chem Eng J. 2008;142:87–94.
[20] Sulaiman F, Abdullah N. Optimum conditions for maximising pyrolysis liquids of oil palm empty fruit bunches. Energy. 2011;36:2352–2359.
[21] Sukiran MA, Kheang LS, Bakar NA, and May CY. Pyrolysis of empty fruit bunches : influence of temperature on the yields and composition of gaseous product. American Journal of Applied Sciences. 2014;11(4):606–610.
[22] Crombie K, Masek O, Sohi SP, et al. The effect of pyrolysis conditions on biochar stability as determined by three methods. GCB Bioenergy. 2013;5:122–131.
[23] Vamvuka D, Kakaras E, Kastanaki E, et al. Pyrolysis characteristics and kinetics of biomass residuals mixtures with lignite . Fuel. 2003;82:1949–1960.
[24] Slopiecka K, Bartocci P, Fantozzi F. Thermogravimetric analysis and kinetic study of poplar wood pyrolysis. Appl Energy. 2012;97:491–497.
[25] Shibata M, Varman M, Tono Y, et al. Characterization in chemical composition of the oil palm (Elaeis guineensis). J Japan Energy Inst. 2008;87:383–388.

[26] Mae K, Hasegawa I, Sakai N, et al. A new conversion method for recovering valuable chemicals from oil palm shell wastes utilizing liquid-phase oxidation with H2O2 under mild conditions. Energy & Fuels. 2000;14:1212–1218.
[27] Abdullah N, Sulaiman F. The properties of the washed empty fruit bunches of oil palm. J Phys Sci. 2013;24 (2):117–137.
[28] Dorez G, Ferry L, Sonnier R, et al. Effect of cellulose, hemicellulose and lignin contents on pyrolysis and combustion of natural fibers. J Anal Appl Pyrolysis. 2014;107:323–331.
[29] Yang H, Yan R, Chen H, et al. Characteristics of hemicellulose, cellulose and lignin pyrolysis. Fuel. 2007;86:1781–1788.
[30] Chen D, Zhou J, Zhang Q. Effects of heating rate on slow pyrolysis behavior, kinetic parameters and products properties of moso bamboo. Bioresour Technol. 2014;169:313–319.
[31] Jiang G, Nowakowski DJ, Bridgwater AV. A systematic study of the kinetics of lignin pyrolysis. Thermochim Acta. 2010;498:61–66.
[32] Pasangulapati V, Ramachandriya KD, Kumar A, et al. Effects of cellulose, hemicellulose and lignin on thermochemical conversion characteristics of the selected biomass. Bioresour Technol. 2012;114:663–669.
[33] De Caprariis B, Santarelli ML, Scarcella M, et al. Kinetic analysis of biomass pyrolysis using a double distributed activation energy model. J Therm Anal Calorim. 2015;121:1403–1410.